RESEARCH

Repeated inhalation of GM-CSF by nonhuman primates induces bronchus-associated lymphoid tissue along the lower respiratory tract

Ryushi Tazawa[1†], Riuko Ohashi[2†], Nobutaka Kitamura[3], Takahiro Tanaka[4], Kazuhide Nakagaki[3], Sachiko Yuki[3], Atsushi Fujiwara[5] and Koh Nakata[3*]

Abstract

Background Repeated inhalation of granulocyte-macrophage colony-stimulating factor (GM-CSF) was recently approved in Japan as a treatment for autoimmune pulmonary alveolar proteinosis. However, the detailed physiological and pathological effects of repeated inhalation in the long term, especially at increasing doses, remain unclear.

Methods In this chronic safety study, we administered 24 cynomolgus monkeys (*Macaca fascicularis*) aged 2–3 years with aerosolized sargramostim (a yeast-derived recombinant human GM-CSF [rhGM-CSF]) biweekly for 26 weeks across four dosing groups (0, 5, 100, and 500 µg/kg/day). We measured the serum GM-CSF antibody (GM-Ab) concentration by an ELISA and assessed the neutralizing capacity of GM-Ab using the GM-CSF-dependent cell line TF-1. We subjected lung tissue samples taken from all monkeys at 27 weeks to histopathological assessment using a sargramostim-specific monoclonal antibody to detect localization of residual sargramostim.

Results All the animals maintained good body condition and showed steady weight gain throughout the study. The pathological analyses of the lung revealed the formation of induced bronchus-associated lymphoid tissue (iBALT) in the lower respiratory tract, even at the clinical dose of 5 µg/kg/day. There was a relationship between the number or size of BALT and sargramostim dose or the serum GM-Ab levels. Immunohistochemical analyses revealed GM-Ab–producing cells in the follicular region of iBALT, with residual sargramostim in the follicles. Leucocyte counts were inversely correlated with GM-Ab levels in the high-dose groups. Additionally, serum GM-Ab from the treated animals significantly suppressed the alveolar macrophage proliferation activity of both Cynomolgus recombinant and rhGM-CSF in vitro.

Conclusion Long-term repeated inhalation of sargramostim led to iBALT formation in the lower respiratory tract, even at the clinical dose of 5 µg/kg/day, with the extent of iBALT formation increasing in a dose-dependent manner. Inhaled sargramostim was localized to the follicular region of iBALT nodules, which may induce the production of GM-Ab.

Keywords Inhalation, GM-CSF, Autoimmune pulmonary alveolar proteinosis, Bronchus-associated lymphoid tissue, Cynomolgus monkey

---

†Ryushi Tazawa and Riuko Ohashi have equally contributed.

*Correspondence:
Koh Nakata
niiiden2012@yahoo.co.jp
Full list of author information is available at the end of the article

Tazawa *et al. Respiratory Research*   (2024) 25:402

Page 2 of 16

Introduction

Granulocyte-macrophage colony-stimulating factor (GM-CSF) is a glycoprotein characterized as a growth factor for granulocyte-macrophage lineages [1]. It promotes the differentiation of stem cells into granulocytes (neutrophils, eosinophils, and basophils) and monocytes, triggers their migration to various tissues, and induces their differentiation into mature macrophages [2–4] and dendritic cells [5]. GM-CSF is released from macrophages, epithelial, and endothelial cells. It supports the local immune system and enhances the function of macrophages and neutrophils, and in the alveolar space, it promotes the terminal differentiation of alveolar macrophages, facilitates surfactant catabolism, and aids the digestion of foreign substances [6].

Sargramostim, a saccharomyces-derived recombinant human GM-CSF (rhGM-CSF), differs slightly from natural human GM-CSF, in that the twenty-third amino acid (Arg) is substituted to Leu. Sargramostim stimulates the proliferation of neutrophils, monocytes, and macrophages after bone marrow transplantation and was developed and approved by the USA Food and Drug Administration as a treatment for granulocytopenia after cancer chemotherapy.

The therapeutic effect of GM-CSF inhalation has been investigated mainly in the context of metastatic lung cancer [7]. A dose-escalation study that investigated metastatic melanoma showed that GM-CSF inhalation induced cytotoxic T lymphocytes in a dose-dependent manner, and that patients tolerated administration of up to 2000 µg of GM-CSF daily [8]. The potential efficacy of sargramostim inhalation as a treatment for pulmonary alveolar proteinosis (PAP) was first suggested in preclinical studies of GM-CSF–deficient mice [9–11] and then tested in open clinical trials for patients with autoimmune PAP (aPAP) [12–14] before being confirmed by two independent randomized double-blinded clinical trials [15, 16]. Recently, the Japanese Ministry of Health, Labor, and Welfare approved the clinical use of sargramostim as an inhalation treatment for aPAP. Previous studies have reported that five days of GM-CSF inhalation improved COVID-19 pneumonia in moderately ill patients [17–19] and suggest that long-term GM-CSF inhalation may be effective in treating pulmonary nontuberculous mycobacteria disease [20]. Even though GM-CSF inhalation therapy will be used to treat various respiratory diseases in the future, a detailed evaluation of its pathophysiological effects has not yet been performed.

Bronchus-associated lymphoid tissue (BALT) is not observed in human adults [21] but is present in about 40% of people aged 2–20 years [22]. It is not constitutively present in all mammals; 100% of rabbits and rats, 50% of guineapigs, and 33% of pigs express BALT, and it is absent in cats [21]. Unlike Peyer's patches, induced BALT (iBALT) often arises in response to stimulation and is known to be a tertiary lymphoid tissue caused by exposure to exogenous microorganisms or endogenous inflammation of the lungs [23]. In humans, iBALT is observed in patients with diffuse panbronchiolitis [24], rheumatoid arthritis [25], and hypersensitivity pneumonia [26]. The structural composition of iBALT resembles the lymphoid tissue described in rabbits and rats, which is characterized by dense encapsulation with lymphocytes arranged in a follicular structure that extends into a network of stromal cells and is located under the airway epithelium, which lacks cilia. BALT shares structural similarities with Peyer's patches in the small intestine and nasal-associated lymphoid tissue. In the airway, BALT occurs at the tracheal bifurcation, where inhaled antigens can become trapped [23]. The iBALT is thought to act as a mucosal immune defense mechanism against exogenous antigens and microorganisms that invade the respiratory tract [27]. Chvatchko et al. observed that peripherally sensitized mice challenged with multiple intratracheal (i.t.) instillations of ovalbumin exhibited the formation of germinal centers within the lung parenchyma, the appearance of follicular dendritic cells bearing ovalbumin, and the emergence of ovalbumin-specific IgG1-, IgE-, and IgA-producing plasma cells [28]. However, there is a lack of published animal studies investigating iBALT formation following long-term inhalation of cytokines.

Before the commencement of a clinical trial aimed at investigating the efficacy and safety of sargramostim inhalation for mild-to-moderate aPAP (PAGE trial, 2016–2018), a nonclinical study was conducted in 2015, using cynomolgus monkeys to confirm the safety of chronic administration of sargramostim for aPAP. The monkeys exhibited good general condition after repeated biweekly inhalation of sargramostim at up to 100 times the clinical dose for 26 weeks, but the pathological examination conducted at 27 weeks revealed increased iBALT even at the clinical dose of 5 µg/kg/day. This study investigated the characteristics of iBALT and discussed its physiological significance.

Materials and methods

Reagents

Sargramostim was provided to Nakata at Niigata University under a Material Transfer Agreement signed between Sanofi Genzyme Corporation and Niigata University.

Animals

The cynomolgus monkeys (*Macaca fascicularis*) were imported from the Primate Quality Control Center of

Tazawa *et al. Respiratory Research*   (2024) 25:402

Page 3 of 16

Table 1 Demographic features of study animals

| Does of inhaled sargramostim (µg/kg/day)	Number of animals (male/female)	Age (weeks) (mean ± SD)	Body weight (kg) (mean ± SD)
0	6(3/3)	185.0 ± 9.3	2.9 ± 0.3
5	6(3/3)	182.8 ± 16.3	3.0 ± 0.3
100	6(3/3)	193.3 ± 23.2	3.1 ± 0.5
500	6(3/3)	185.0 ± 14.8	3.1 ± 0.6

Ina Research Philippines. Three-year-old males ($n = 12$) and three- or four-year-old females ($n = 12$) were used for the experiments in the present study. Hematoxylin-and-eosin-stained specimens from the lungs of four other healthy monkeys were examined as control specimens for lungs without sargramostim inhalation. All animal experiments were performed by Ina Research (Nagano, Japan), an institution that is fully accredited by the Association for Assessment and Accreditation of Laboratory Animal Care International, with approval by the Institutional Animal Care and Use Committee (IACUC, approval no. 15091) of Ina Research and the Animal Experimental Ethics Board (approval no. 27-102-1) of Niigata University. All animal experiments followed the National Institutes of Health's guide for the care and use of laboratory animals (NIH Publications No. 8023, revised 1978).

Assignment to experimental groups

Each of the monkeys was classified according to its body weight and randomly assigned to one of four dosing groups (0, 5, 100, or 500 µg/kg/day) using the Provantis system (Table 1). The animals in each group were numbered randomly in each group.

Administration of sargramostim

The four dosing groups comprised six monkeys each (three males and three females; Fig. 1. Each animal was restrained in a monkey chair and a custom-made inhalation mask was applied. The mask was connected to a Pari LC Sprint Star Nebulizer (Pari, Starnberg, Germany), through which 1.5 mL of sargramostim solution was administered. The sargramostim solution (0, 5, 100, or 500 µg/kg/day in a tris/mannitol/sucrose solution at 1.2/40/10 g/L) was inhaled until it was fully depleted. This procedure was conducted daily in the first week of each two-week cycle, and administration was suspended during the second week. These two-week cycles were repeated for a total of 26 weeks.
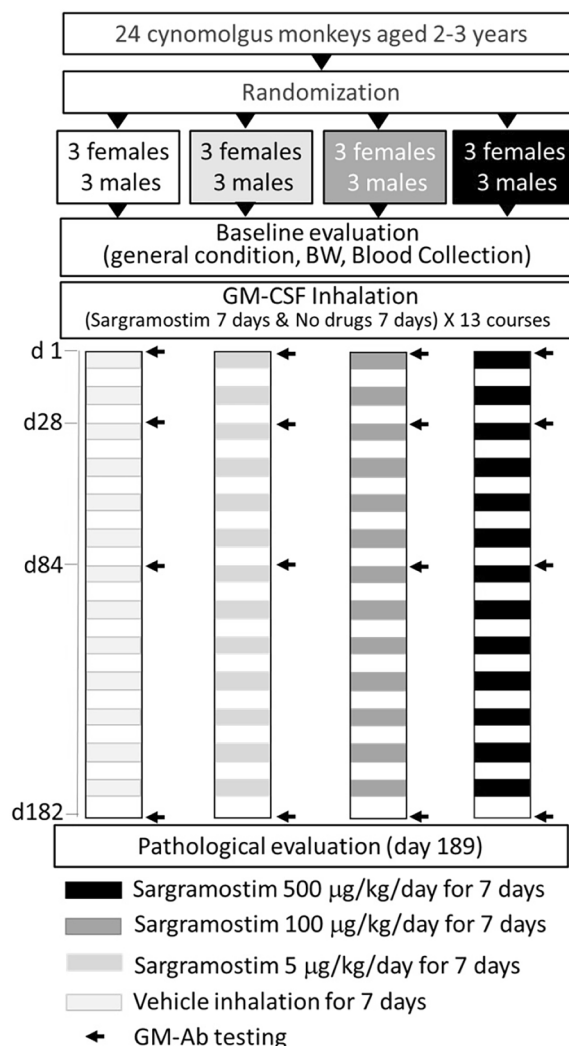
Fig. 1 Profile of the study cohort showing the administration schedule of aerosolized sargramostim or vehicle to 24 cynomolgus monkeys. The monkeys, of which 12 were males and 12 females, were divided into four groups: vehicle and sargramostim at 5 µg/kg/day, 100 µg/kg/day, or 500 µg/kg/day. The drug was administered via inhalation for 13 cycles over 26 weeks. Blood was collected from all monkeys at baseline and on days 8, 28, 82, and 176 for blood biochemical tests. In addition, autopsies were performed two weeks after the end of inhalation (day 189) for pathological evaluation

Study procedure

The general condition, food intake, and body weight of each animal were assessed twice daily, once daily, and once weekly, respectively. Electrocardiography, blood pressure measurement, and ophthalmic examination were performed at baseline (days −7–1), 13 weeks (day 91–98), and 25 weeks (day 176–182) (Table 2). Hematological and biochemical testing were carried out on days 1 (C-reactive protein only), 3, 8, 92, and 176. The

Tazawa *et al. Respiratory Research*   (2024) 25:402

Page 4 of 16

Table 2 Examination schedule for a 26-week toxicity study of chronic sargramostim inhalation

Item	Frequency and timing of examination
General condition	Twice daily
Food uptake	Once daily
Body weight	Once weekly
Heart rate/min	Pre- and post-inhalation at day 1, week 13 and 25
Blood pressure	Pre- and post-inhalation at day 1, week 13 and 25
Electrocardiogram	Pre- and post-inhalation at day 1, week 13 and 25
Ophthalmology test	Pre-inhalation and week 13 and 25
Hematological test	Day -3, 8, 92, and 176
Clinical chemistry	Day -3, 8, 92, and 176
Urinalysis	Weeks -1, 13, and 25
Autopsy	Week 27

concentration of anti-GM-CSF antibody (GM-Ab) in the serum was measured using an enzyme-linked immunosorbent assay (ELISA) method as previously described [12, 14, 15]. The neutralizing capacity of GM-Ab was measured via a GM-CSF bioactivity assay using TF-1 cells, a GM-CSF-dependent cell line [29].

Histopathological examination

Eight days after the final administration of the drug, all monkeys were euthanized, via thiopental overdose, and autopsies were performed. After the organs that had been extracted during autopsy had been weighed, they were fixed with 10% neutral-buffered formalin solution, embedded in paraffin, and sectioned at 3 μm thickness for histopathological examination with hematoxylin and eosin staining. Paraffin-embedded sections of lung tissue from the four healthy monkeys without a history of inhalation of any drug served as controls. The lung tissue samples used for the histopathology were randomly chosen during the autopsy, with section areas ranging from 122.6 mm^2 to 396.3 mm^2. To evaluate the degree of BALT nodule formation, nodular lymphocytic aggregations with more than 50 lymphocytes were counted and measured. The samples were screened at low-power magnification (40×), and five fields at 100× magnification (10× objective lens and 10× eyepiece with field number 22, one field ≈ 3.8 mm^2, five fields ≈ 19 mm^2) were selected in order of the area occupied by BALT nodules in the peribronchial, peribronchiolar, and alveolar regions. The sizes of BALT nodules were categorized, based on the minor axis diameter, into the following classes: class 1, 50–100 μm; class 2, 100–200 μm; class 3, 200–300 μm; class 4, 300–400 μm; and class 5, ≥ 400 μm.

Immunohistochemistry

For the immunohistochemistry, the sections were deparaffinized and subjected to heat-induced epitope retrieval (HIER) in Histofine antigen retrieval buffer, pH 9 (Nichirei Bioscience, Tokyo, Japan). After endogenous peroxidase blocking with 0.3% hydrogen peroxide in methanol for 30 min, the sections were blocked with 10% normal goat serum in phosphate-buffered saline (PBS) for 30 min, then incubated with anti-sargramostim monoclonal antibody (clone 40–1 H; generated as previously reported [29]; 4 μg/mL) anti-CD21 antibody (EP3093; Abcam; 1:8000 dilution), and anti-CD3 antibody (Dako clone F7.2.38; Agilent Technologies, Santa Clara, CA; 1:200 dilution) at 4 °C overnight, followed by washing with PBS and incubation with Histofine Simple Stain MAX-PO (MULTI) kit (#424152, Nichirei Biosciences, Tokyo, Japan) for 30 min at room temperature. Anti-sargramostim monoclonal antibody (clone 40–1 H) was generated as previously reported [30]. To visualize the localization of GM-Ab, sections were subjected to HIER in Histofine antigen retrieval buffer, pH 6 (Nichirei Bioscience), then treated with 3% hydrogen peroxide for 30 min. Next, sections were treated with Endogenous Biotin-Blocking Kit (E21390, Thermo Fisher Scientific, Waltham, MA) according to the manufacturer's instructions, followed by incubation in 10% normal goat serum in PBS for 30 min, and then overnight incubation with 500 ng/mL of biotin-conjugated rhGM-CSF [31] in 10% normal goat serum in PBS at room temperature. Sections were then washed with PBS and incubated with HRP-conjugated streptavidin (Thermo Fisher Scientific) for 50 min at room temperature. After washing, signals were visualized with a Histofine Diaminobenzidine (DAB) Substrate Kit (Nichirei bioscience) and counterstained with hematoxylin. Whole-slide images were obtained using a NanoZoomer S210 digital slide scanner (Hamamatsu Photonics, Hamamatsu, Japan). The number and size of the germinal centers in the hilar lymph nodes were evaluated using the NDP.view2 software (Hamamatsu Photonics).

To visualize the localization of anti-GM-CSF antibody, Alexa Fluor™ 488 Tyramide SuperBoost™ Kit, streptavidin (B40932, Thermo Fisher Scientific, Waltham, MA) was used according to the manufacturer's instruction. Deparaffinized sections were subjected to HIER in Histofine antigen retrieval buffer, pH 9 (Nichirei Bioscience, Tokyo, Japan), Endogenous Biotin-Blocking Kit (E21390, Thermo Fisher Scientific, Waltham, MA), and then incubated overnight with biotin-conjugated rhGM-CSF (500ng/ml) and Polyclonal Rabbit Anti-Human IgG (prediluted, Dako IR512; Agilent Technologies, Santa Clara, CA) or Polyclonal Rabbit Anti-Human IgA (prediluted, Dako IR510; Agilent Technologies, Santa Clara, CA) at

Tazawa *et al. Respiratory Research*   (2024) 25:402

Page 5 of 16

Table 3 Counts of white blood cells (10^3 cell/μl) during repeated GM-CSF inhalation

Male (mean ± SD) Does (µg/kg/day)	Baseline	Day 8	Day 92	Day 176
0 (n = 3)	11.22 ± 1.46	9.96 ± 2.42	10.00 ± 1.55	10.59 ± 1.07
5 (n = 3)	10.56 ± 1.96	9.21 ± 2.17	8.28 ± 1.43	8.88 ± 1.54
100 (n = 3)	10.23 ± 1.27	11.03 ± 1.30	11.64 ± 0.90	12.10 ± 3.81
500 (n = 3)	7.51 ± 1.78	18.67 ± 3.21	8.26 ± 0.83	8.87 ± 1.45
Female (mean ± SD) Does (µg/kg/day)	Baseline	Day 8	Day 92	Day 176
0 (n = 3)	8.61 ± 1.14	7.70 ± 0.84	8.64 ± 1.97	7.88 ± 0.14
5 (n = 3)	9.56 ± 1.75	7.72 ± 1.69	7.69 ± 1.76	7.45 ± 0.82
100 (n = 3)	10.54 ± 2.32	9.14 ± 1.87	9.88 ± 1.40	10.49 ± 1.66
500 (n = 3)	6.12 ± 1.02	24.54 ± 1.87	6.43 ± 1.24	6.08 ± 1.73

room temperature. Signals were detected with Alexa Fluor™ 488 Tyramide SuperBoost™ Kit, streptavidin (Thermo Fisher Scientific) and F(ab')2-Goat anti-Rabbit IgG (H + L) Cross-Adsorbed Secondary Antibody, Alexa Fluor Plus 555 (Catalog A48283, Thermo Fisher Scientific, Waltham, MA, 1:500 dilution). Slides were mounted with VECTASHIELD mounting medium with DAPI (Vector Laboratories, Burlingame, CA). Images were captured using a confocal laser scanning microscope (LSM810; Carl Zeiss, Jena, Germany).

Suppression of GM-CSF-dependent alveolar macrophage proliferation by cynomolgus monkey serum

Alveolar macrophages (1.3×10^4/well) were purified from bronchoalveolar lavage fluid obtained using a bronchofiberscope (BF type XP60, Olympus, Tokyo, Japan) from a monkey other than those used for sargramostim preclinical inhalation. The cells were seeded into each well of several 96-well plates (Cellstar 96-Well Cell Culture Plate, Greiner Bio-One, Frickenhausen, Germany). After washing the plate twice with PBS to remove nonadherent cells, the adherent cells were incubated for three days in the presence or absence of the GM-Ab–containing monkey serum collected on day 176 and 1 ng/mL of sargramostim or cynomolgus monkey recombinant GM-CSF (Biotech, Oklahoma City, OK). The cells were pulsed with 100 µM bromodeoxyuridine (BrdU) for an additional 20 h. The quantity of BrdU incorporated was measured using a cell-proliferation ELISA (Roche Diagnostics GmbH, Mannheim, Germany). The stimulation index was calculated from the ratio of incorporated BrdU in cells incubated with sargramostim to those without sargramostim.

Statistical analysis

For each measurement, continuous variables were expressed as mean ± SD or median [25%, 75%] and discrete variables were expressed as proportions (%). Due to the presence of several outliers or non-normally distributed data for some variables, we investigated the relationship between continuous variables using Spearman's rank correlation coefficient. The discrete variable percentages were compared among groups using χ^2 or Fisher's exact tests. For multiple group comparisons, due to the homogeneity of variance was assessed by the Levene test, we used the one-way ANOVA, followed by the Bonferroni correction for multiple comparisons. A generalized estimating equation was used to evaluate prognostic factors, with the target observations as the dependent variables and background variables as the independent variables. The model accounted for the correlation in within-subject repeated data. Analyses were performed using Excel version 14 (Microsoft, Redmond, WA), SAS software version 9.4 (SAS Institute, Cary, NC), IBM Statistics 28.0.1.1 (IBM, Armonk, NY), and R software version 4.0.0 (R Development Team).

Results

General condition and bloodwork

Throughout the experimental period, all monkeys exhibited good appetite and nutrition, underwent normal weight gain, and showed normal behavior. No deaths were recorded during the study. Blood chemical tests, blood coagulation tests, urinalysis, electrocardiography, blood pressure, and ophthalmic examinations at baseline, 13, and 25 weeks revealed no abnormalities. In the 500 µg/kg group, the WBC count increased rapidly by Day 8, but then decreased again (Table 3). No significant changes were observed over time in the other dose groups. No clear relationship was observed between

Tazawa *et al. Respiratory Research*   (2024) 25:402

Page 6 of 16

dose and WBC count. However, for both male and female monkeys receiving the two highest doses (100 and 500 μg/kg/day), neutrophil and eosinophil counts were significantly elevated on day 8 compared to baseline. These counts subsequently declined, with only eosinophils being elevated on days 92 and 176 in the 100 μg/kg/day group compared to other groups.

iBALT hyperplasia

There were no differences in mean lung weight between the four dosing groups at autopsy. Microscopic evaluation revealed iBALT hyperplasia in the peribronchial, peribronchiolar, and perialveolar regions (Fig. 2A–C). The number of peribronchial iBALT nodules per 19 mm^2 of examined lung was not affected by the sargramostim dose (Fig. 2D, the left panel). However, in both peribronchiolar and perialveolar regions (Fig. 2D, the middle and right panel, respectively), the number of iBALT nodules increased dose-dependently. The correlation between dose and number of nodules was strong, with ρ=0.74 (Spearman, $P < 0.001$) for the former and 0.80 (Spearman, $P < 0.001$) for the latter. A generalized linear model with the number of iBALTs as the objective variable revealed that the interaction between site, dose, and gender was significant ($P = 0.016$, Supplemental Fig. 2, Supplemental Table 1). In other words, there were gender differences in the number of iBALTs depending on the site and dose, and in particular, for peribronchial doses of 0, 100, and 500 μg, male had more iBALT than female. There were no gender differences in the size of iBALT depending on site or dose (Supplemental Fig. 3, Supplemental Table 2). When the BALT count was compared between the four dose groups using one-way analysis of variance, a significant difference was observed among the four groups ($P < 0.001$) in peribronchiolar and alveolar region, but not in the peribronchial region. When multiple testing was performed, significant differences were observed between all groups: 0 μg and 5 μg, 0 μg and 100 μg, and 0 μg and 500 μg, with 0 μg showing the smallest value in both the peribronchiolar and perialveolar region, but not in the peribronchial region. Similarly, a one-way analysis of variance was used to compare the size of BALT among the four dose groups, and no significant difference was found among the four groups in both the peribronchial and peribronchiolar regions but a significant difference was observed among the four groups ($P = 0.001$) in the alveolar region. When multiple testing was performed, no significant difference was observed between any groups in both the peribronchial and peribronchiolar regions but a significant difference was observed between

all groups: 0 μg and 5 μg, 0 μg and 100 μg, and 0 μg and 500 μg, with 0 μg showing the smallest value.

When the sizes of BALT nodules were categorized, based on the minor axis diameter, into the following classes: class 1, 50–100 μm; class 2, 100–200 μm; class 3, 200–300 μm; class 4, 300–400 μm; and class 5, ≥ 400 μm, the size of peribronchial iBALT was not affected by the sargramostim dose (Fig. 2E, the left panel), but in both peribronchiolar and perialveolar regions (Fig. 2E, the middle and right panel, respectively), it also appeared to increase in a dose-dependent manner, reaching a plateau more than 100 μg/kg/day. The degree of iBALT formation in the four control animals (no inhalation) was similar to that of the monkeys in the vehicle-inhalation group. Thus, the effects of inhaled sargramostim on lung pathology were airway region-specific and dose dependent. Additionally, it strongly suggests that this is a biological response to inhaled sargramostim. Thus, the number and size of iBALT in peribronchiolar and perialveolar regions appeared to depend on the dose of inhaled sargramostim. With vehicle alone, iBALT was formed only in the peribronchial region, but as the dose of sargramostim increased, iBALT around the peribronchiolar and perialveolar regions increased and got larger (Fig. 2F). The increased iBALT in peribronchiolar and perialveolar regions suggests that it might be a host response to stimulation by sargramostim.

Localization of the anti-sargramostim antibody-producing cells in iBALT and other lymphatic organs

Since iBALT increased in number and size in a dose-dependent manner as described above, we suspected that the iBALT was producing antibodies against inhaled sargramostim. Therefore, we focused on the lungs of monkeys of the 500 μg/kg/day group, where the number and size of BALT increased mostly. Using immunohistochemistry with biotinylated GM-CSF, we identified the site of anti-sargramostim antibody production as all iBALT nodules in the peribronchial, peribronchiolar, and perialveolar regions in the 500 μg/kg/day group (Fig. 3A–F). Using hematoxylin as a counterstain, both primary lymphoid follicles and secondary lymphoid follicles with germinal centers were observed in each iBALT nodule in the peribronchial, peribronchiolar, and perialveolar regions. Most cells in the primary follicles showed anti-sargramostim antibody production (Fig. 3E). In the secondary follicles, anti-sargramostim antibody production was observed diffusely in the germinal center. Weaker but diffuse anti-sargramostim antibody production was observed in the mantle zone and the subepithelial
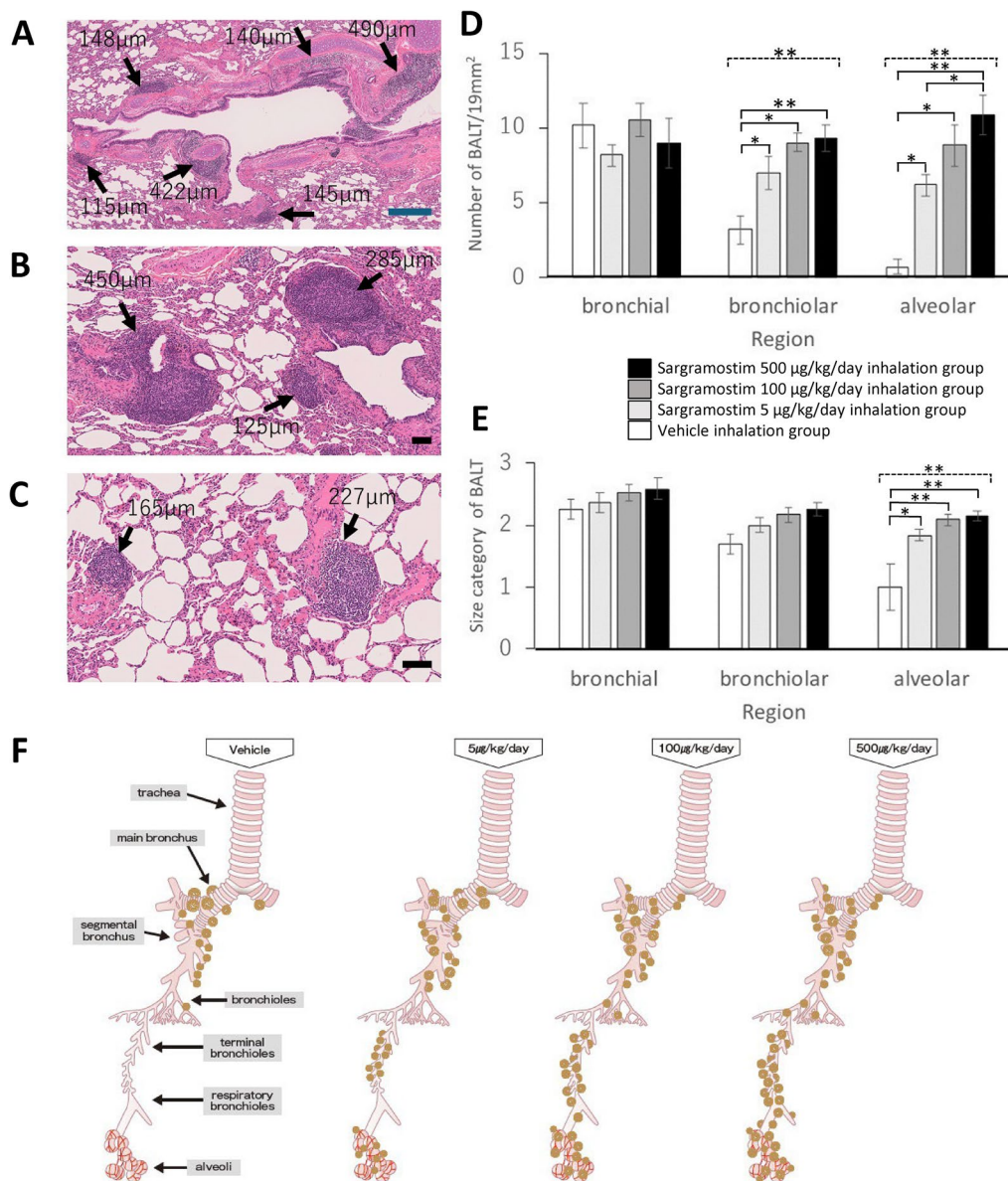
Fig. 2 Lung histology at day 189 for monkeys that received sargramostim via inhalation (stained with hematoxylin and eosin). **A** Lung sections including bronchus with bronchial cartilage from a monkey in the 100 µg/kg/day group. The size and number of BALT nodules along the bronchus of this individual is comparable to those in the vehicle-treated control group. Representative microphotographs of BALT hyperplasia along the bronchioles from a monkey in the 100 µg/kg/day group (**B**) and along the alveolar ducts from a monkey in the 500 µg/kg/day group (**C**). Black arrows indicate BALT; Blue scale bar: 500 µm; black scale bars: 100 µm. **D, E** The effect of the dosage of inhaled sargramostim on the number per 19 mm 2 and the mean size category of BALT formation in lung tissues in monkeys. Data presented are mean ± SD. Based on the minor axis diameter, the size of BALT was categorized into the following classes: class 1, 50–100 µm; class 2, 100–200 µm; class 3, 200–300 µm; class 4, 300–400 µm; and class 5, ≥ 400 µm. **F** Schematic diagram of BALT formation in cynomolgus monkeys administered vehicle and sargramostim at 5,100 and 500 µg /kg/day by inhalation every other week for 26 weeks. After vehicle inhalation, BALT was observed only in the bronchial region. As shown in (**D**) and (**E**), the number and size of iBALT in the bronchiolar and alveolar regions were increased in the sargramostim inhalation administration group as the dose increased. Multiple comparison tests (bracket in solid line) were conducted between the treatment groups, and a one-way analysis of variance (bracket in broken line) was conducted for each region (*; p < 0.05, **; p < 0.01)

area outside the follicles (Fig. 3A–D). In the serial sections, most cells in the iBALT nodules' primary follicles and germinal centers with a surrounding mantle layer of secondary follicles were positive for CD21, indicating the presence of B cells or follicular dendritic cells. Scattered CD3-positive T cells were observed in all iBALT nodules

Tazawa *et al. Respiratory Research*   (2024) 25:402

Page 8 of 16

(data not shown). In the hilar lymph nodes, signals that were too faint for photography were observed visually in some lymphoid follicles. In contrast, no anti-sargramostim antibody production was detected in the lungs of individuals in the vehicle group or in either groups' spleens. We found distinct colocalized cells of anti-GM-CSF antibody and IgG or IgA within CD21-positive B cell region of iBALT from the alveolar or peribronchiolar regions of sargramostim-treated monkeys by double immunofluorescence with anti-IgG, anti-IgA, and biotin-conjugated rhGM-CSF and confocal microscopy (Fig. 3G).

Sargramostim accumulation in iBALT nodule germinal centers

An accumulation of sargramostim, detected using a sargramostim-specific monoclonal antibody [30], was confirmed in the germinal centers in iBALT nodules in the monkeys that received 500 µg/kg/day of sargramostim (Fig. 4A–C). This antibody specifically recognizes the third to thirty-second residues of the sargramostim peptide, including the substituted twenty-third amino acid (Arg to Leu), but not the original peptide [30]. Accordingly, the detection of sargramostim in the germinal centers did not arise from a nonspecific reaction, as confirmed by the absence of sargramostim in the BALT of vehicle-treated monkeys (Fig. 4D). Further, sargramostim was also detected in the germinal centers of the hilar lymph nodes (Fig. 4E) but not in the spleen of monkeys receiving the 500 µg/kg/day dose (Fig. 4F). The fact that iBALT was detected in the autopsied lungs two weeks after the last inhalation of sargramostim indicates the prolonged retention time of inhaled sargramostim.

Correlation between serum GM-Ab concentration and iBALT density

We detected IgG-type GM-Ab on day 28 in 13 of the 18 monkeys that received sargramostim (Fig. 5A), and in all 18 monkeys on days 84 and 182. Over the 26-week inhalation period, the concentration of GM-Ab increased in a dose-dependent manner. The time course

of IgA-type GM-Ab was quite similar to that of IgG-type GM-Ab, although a quantitative comparison was precluded by the lack of a standard IgA-type antibody. Nevertheless, the dose dependency of serum IgA-type GM-Ab was confirmed (Fig. 5B). Likewise, neutralizing capacity, which was expressed as the serum dilution titer required to suppress TF-1 cell proliferation by 50%, increased over time in a dose-dependent manner. The titer ranged from approximately 10–100× on day 28 to 200–22,400× on day 182, corresponding to a 50% inhibition of 0.5 ng/mL sargramostim bioactivity (Fig. 5C). Interestingly, the specific activity of the neutralizing antibody, which was defined as the neutralizing capacity per 1 µg of IgG type-GM-Ab, increased from day 84 to 182 but did not differ between the three dosing groups on these days (Fig. 5D). If GM-Ab is produced in iBALT, its concentration should be positively correlated with the size and number of iBALT nodules. Indeed, the density of iBALT at the time of autopsy (day 189) was correlated with both the serum IgG-type GM-Ab concentration (Fig. 5E, $\rho = 0.752$, $P < 0.001$) and neutralizing ability (Fig. 5F, $\rho = 0.736$, $P < 0.001$) at day 182 in the 100 and 500 µg/kg/day groups. Similarly, the size of iBALT was correlated with both the serum IgG-type GM-Ab concentration (Fig. 5G, $\rho = 0.528$, $P = 0.008$) and neutralizing ability (Fig. 5H, $\rho = 0.423$, $P = 0.039$). These results also strongly suggest that the GM-Ab was produced in iBALT. Using a generalized estimating equation with IgG, IgA type GMAb, and neutralizing capacity as the objective variable, the interaction between dose and day was significant ($P < 0.001$). In other words, there was a significant difference in the pattern of change over time in IgG, IgA type GMAb, and neutralizing capacity between doses, with 500 µg having the highest rate of increase, followed by 100 µg, 5 µg, and vehicle.

Function and cross-reactivity of serum GM-Ab

The proliferation of alveolar macrophages in vitro was measured via cellular incorporation of BrdU. Serum with higher concentrations of GM-Ab strongly inhibited BrdU

(See figure on next page.)

Fig. 3 Immunohistochemical detection of putative anti-GM-CSF antibody producing cells in the BALT from the bronchial (**A, B**), bronchiolar (**C, D**), and alveolar (**E, F**) areas of sargramostim-treated monkeys. Low-magnification (A, C, scale bars: 200 µm) and high-magnification (**B, D, E, F**, scale bars: 50 µm) images of the areas of lung sections showing the BALT nodules along the bronchus (Br) with bronchial cartilage (indicated by an asterisk) and the bronchioles (br). The panels (**B**) and (**D**) are high-magnification images of the areas indicated by rectangles in the panels (**A, C**), respectively In the secondary follicles, anti-sargramostim antibody production was observed diffusely in the germinal center. Weaker but diffuse anti-sargramostim antibody production was observed in the mantle zone and the subepithelial area outside the follicles (**A–D**). Most cells in the primary follicles showed anti-sargramostim antibody production (**E**) Panel (**G**) shows representative confocal microscopy images of double-immunofluorescence stained with biotin-conjugated rhGM-CSF (green), anti-IgG or anti-IgA antibody (red), and merged image of the iBALT from the alveolar or peribronchiolar regions of sargramostim-treated monkeys. Scale bar, 2 µm. All slides were counterstained with DAPI (blue) for nuclear staining
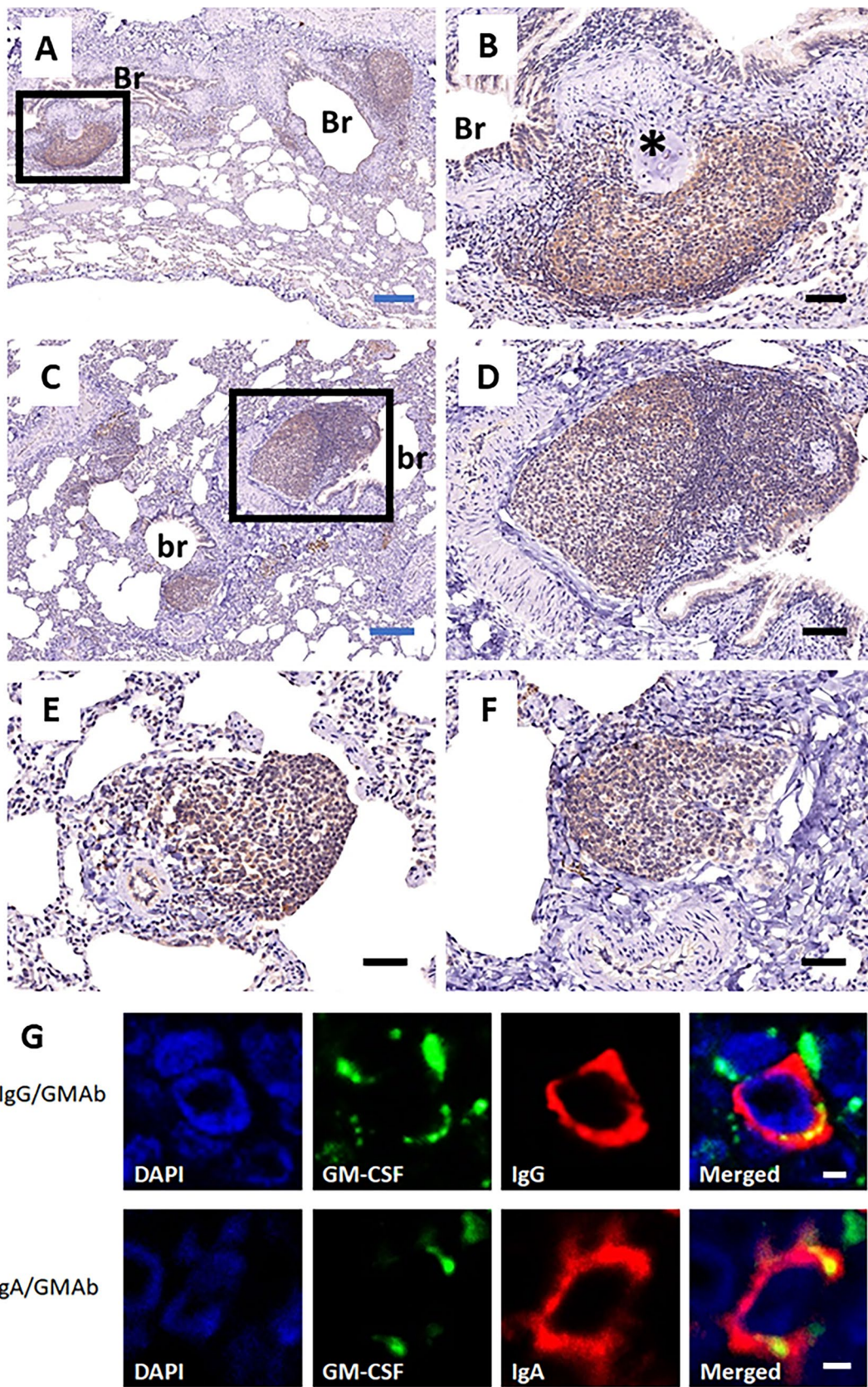
**Fig. 3** (See legend on previous page.)
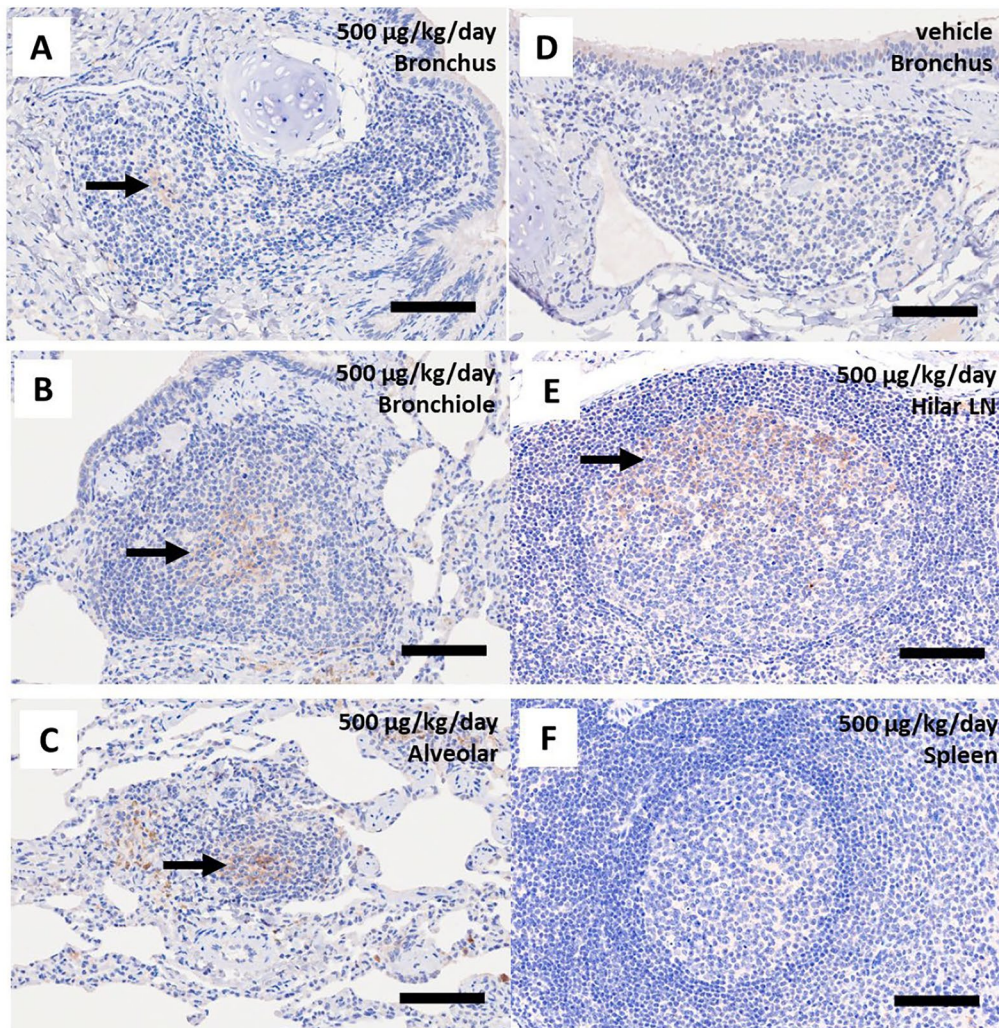
Fig. 4 Detection of residual sargramostim using sargramostim-specific monoclonal antibody (clone 40–1 H). Residual sargramostim was observed in the BALT of cynomolgus monkeys receiving 500 µg/kg/day of sargramostim by inhalation. The bronchial (**A**), bronchiolar (**B**), and alveolar regions (**C**), respectively, were strongly stained. No positive staining was observed in BALT from vehicle-treated monkeys (**D**). Sargramostim was also detected in the germinal centers of the hilar lymph nodes (**E**) but not in the spleen (**F**) of monkeys receiving 500 µg/kg/day of sargramostim via inhalation. Scale bars: 100 µm

uptake in cynomolgus alveolar macrophages incubated with sargramostim or cynomolgus monkey GM-CSF, indicating that serum GM-Ab cross-reacted with cynomolgus GM-CSF (Fig. 6A). The effect of the neutralizing antibody on the living organisms in vivo was particularly evident in our observation of emerging correlations in the 500 µg/kg/day group between peripheral white blood cell counts and antibody concentrations (Fig. 6B, $\rho = -0.573$, $p = 0.051$) or neutralizing capacities (Fig. 6C, $\rho = -0.650$, $p = 0.022$), while this inverse correlation was not observed in the vehicle-treated, 5 µg/kg/day, or 100 µg/kg/day groups. These results suggest that the amount of anti-GM-CSF antibodies and neutralizing ability induced by 500 µg/kg/day sargramostim inhalation reached a level sufficient to suppress leucogenesis in vivo.

Discussion

This study shows that repeated inhalation of sargramostim over 26 weeks induced BALT formation in the lower respiratory tract of cynomolgus monkeys in a dose-dependent manner. Immunohistochemical analysis revealed the presence of anti-GM-Ab producing cells and sargramostim in the follicular region of iBALT, suggesting that the inhaled sargramostim could be transported from the airway to the iBALT follicles, triggering GM-Ab production. However, no alveolar proteinosis was observed
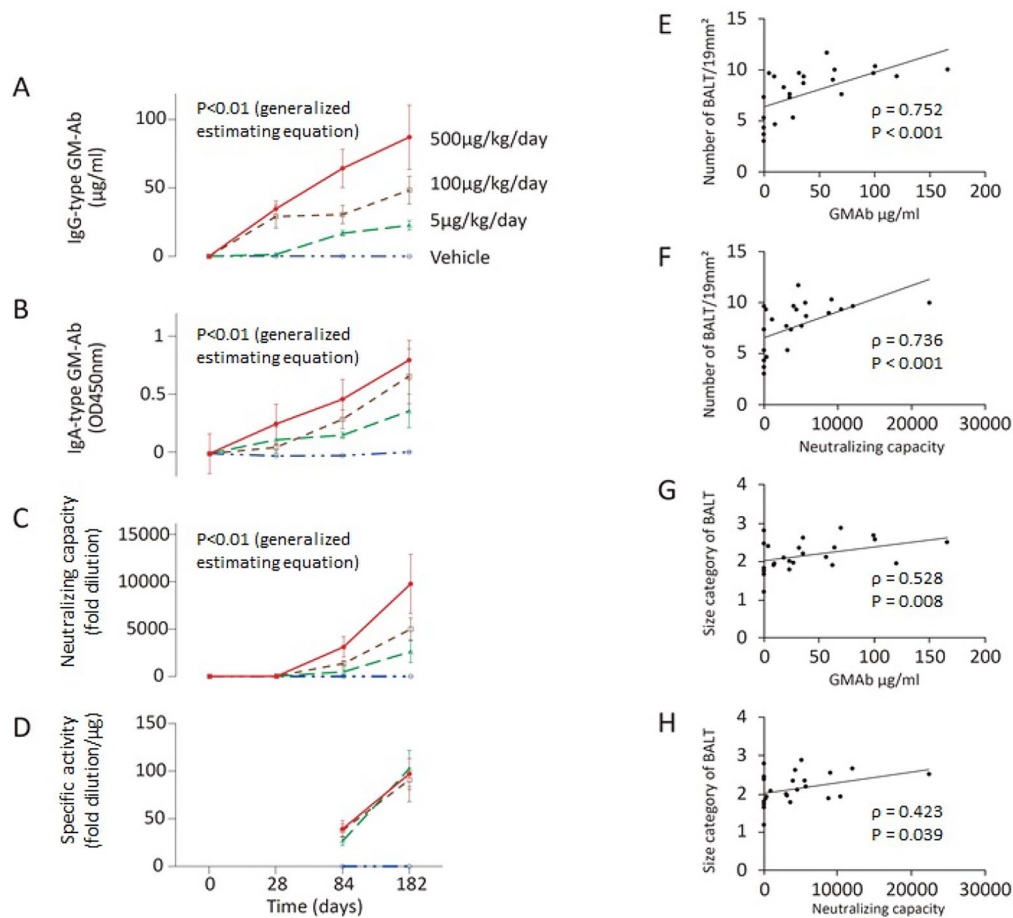
Fig. 5 Time-course of serum levels of IgG-type anti-GM-CSF antibodies (**A**), titer of IgA-type GM-Ab measured via enzyme-linked immunosorbent assay for IgA-type GM-Ab at OD450 nm (**B**), titer of neutralizing capacity (**C**), and specific activity (**D**). Data presented are mean ± SD. Panels E–H show the correlation of the concentration of antibodies with the size and number of iBALT nodules. The density of iBALT at the time of autopsy (day 189) was correlated with both the serum IgG type GM-Ab concentration (**E**) and neutralizing ability (**F**) at day 182 in the 100 and 500 μg/kg/day groups. Similarly, the size of iBALT nodules was correlated with both serum IgG type GM-Ab concentration (**G**) and neutralizing ability (**H**)

in any of the monkeys. This may mean that GM-Ab was produced, but at the same time GM-Ab could not completely abrogate the function of alveolar macrophages, not fully antagonizing the action of excessive GM-CSF that entered the alveoli through inhalation. The leukocytosis effect of sargramostim occurs transiently by Day 8 in the 500 μg/kg/day group, but when the production of GM-Ab increases after Day 28, it becomes more pronounced than the hematopoietic effect.

The dose-dependent increase in iBALT along the lower respiratory tract of cynomolgus monkeys receiving chronic GM-CSF inhalation differs from the iBALT observed in human smokers, which is typically found in the bronchial region [32], and the BALT structures of human infants, which develop around the major airway during the first three years of life [33]. Instead, it resembles the bronchiolitis and iBALT observed in rhesus monkeys in response to subacute exposure to high

concentrations of magnesium sulfate [34]. The skewed distribution in the lower respiratory tract may be caused by the deposition site of the drug mist and its transport via airway surface fluids. Specifically, the drug mist containing sargramostim may become entrapped in airway surface fluids upon reaching the distal respiratory bronchiole region, and thereby transported through the alveoli into the lymphatic vasculature, where it contributes to BALT formation. Conversely, drug mist deposited in the trachea and proximal bronchial region may be eliminated upwards via the ciliary movement of the respiratory tract. The peribronchial BALT observed in this study regardless of dose groups may have been formed by the airway immune defense system against exogenous various antigens (other than GM-CSF) that were inhaled and trapped in proximal bronchial bifurcation.

If iBALT were induced by the physiological effects of GM-CSF, how would we explain the creation of GM-CSF
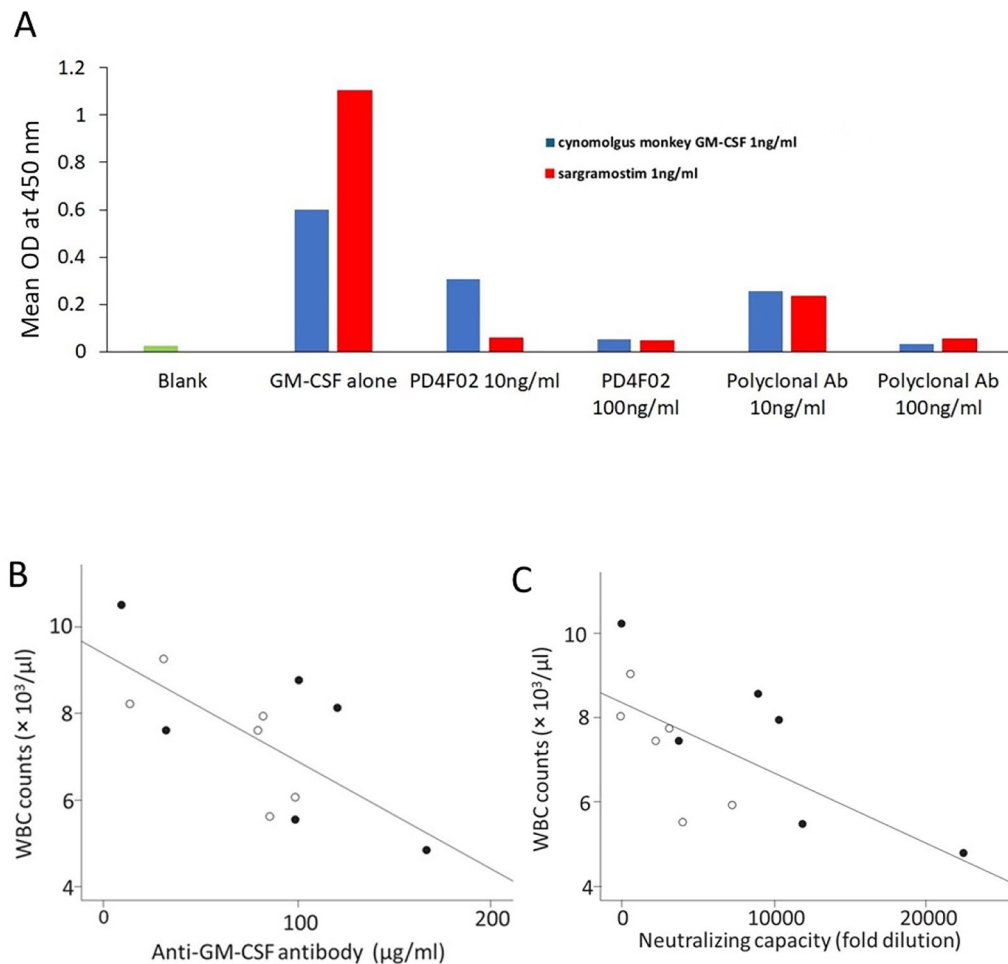
Fig. 6 A The cross-reactivity of serum GM-Ab with cynomolgus GM-CSF was evaluated by inhibition of in vitro proliferation of alveolar macrophages measured via cellular incorporation of BrdU. Serum with increased GM-Ab concentration as well as polyclonal anti-GM-CSF antibody 10 ng/ml and 100 ng/ml, strongly inhibited in vitro proliferation of cynomolgus alveolar macrophages incubated with sargramostim (red bar) or cynomolgus monkey GM-CSF (blue bar). (**B** and **C**) Correlation scatter plots between white blood cell counts and serum GM-Ab levels (**B**) or titer of neutralizing capacity (**C**) are also provided for days 84 (O) and 182 (●). There were correlations in the 500 μg/kg/day group between peripheral white blood cell counts and antibody concentrations **B**, $\rho = -0.573$, p =0.051) or neutralizing capacities **C**, $\rho = -0.650$, p =0.022)

specific antibodies in iBALT? It is unlikely a physiological effect, because GM-CSF specific antibody production occurred. Given that the GM-CSF of cynomolgus monkeys differs from sargramostim by six amino acids, it is reasonable to expect that sargramostim would be recognized as a foreign substance and trigger antibody production. However, anti-cynomolgus monkey GM-CSF antibodies would probably also have been generated in response to the administration of a considerable amount of cynomolgus monkey GM-CSF via inhalation over an extended period. Indeed, subcutaneous administration of recombinant human GM-CSF readily induces GM-Ab in cancer patients [35]. It is believed that the induction of autoantibodies against cytokines may stem from the presence of cytokine-responsive B cell clones. Our findings indicate that there are very few B-cell clones in healthy subjects that produce GM-CSF–binding antibodies [36]. Nevertheless, such clones may be stimulated by exogenous GM-CSF to undergo somatic hypermutations and class switching to produce IgG-type GM-Ab. Using several experimental approaches, we previously reported the detection of GM-Ab in all healthy subjects evaluated at low levels sufficient to rheostatically regulate multiple myeloid functions [37]. Under steady-state conditions, more than 99% of serum GM-CSF was bound and neutralized by GM-CSF autoantibody in healthy individuals, which may mask the presence of GM-Ab and obscure its function.

Tazawa *et al. Respiratory Research*   (2024) 25:402

Page 13 of 16

In GM-CSF inhalation therapy for PAP, patients exhibited an increase in GM-Ab concentration, but the neutralizing capacity of GM-Ab remained unchanged during treatment [16]. The GM-Ab may significantly suppress the physiological activity of extrinsic GM-CSF in patients with PAP, with limited stimulation of GM-Ab production. The therapeutic dose for aPAP patients is 250 μg/day, which is consistent with the 5 μg/kg/day group in this study. Even at this dose, significantly more BALT was formed in the lower respiratory tract than in vehicle-inhaled monkeys, and the antibody production also increased, so it seems that BALT formation and antibody production occur at clinical doses to humans. In APAP patients, due to the presence of GM-CSF autoantibodies, GM-CSF inhalation might cause minimal changes. However, in the context of GM-CSF inhalation as a long-term therapy for nontuberculous mycobacteria disease in patients lacking GM-Ab, BALT may be induced and the subsequent antibody production may occur. High-resolution computed tomography can detect follicular bronchiolitis in patients with diffuse panbronchiolitis, rheumatoid arthritis, and Sjogren syndrome [38–41], and it may also be able to detect BALT. The maximum diameter of BALT observed in cynomolgus monkeys in both the present study and in other studies was 0.4 mm [42–44]. Consequently, incidental observations of BALT may arise during diagnostic procedures such as transbronchial cryo-biopsy or surgical biopsy of the lungs.

The duration of GM-CSF exposure may play a crucial role in BALT formation. On day 28, serum GM-Ab concentrations were low and neutralizing capacity was not detected in all monkeys. However, neutralizing capacity was observed in almost all treated animals (except for one monkey in 100 μg/kg/day sargramostim group) on day 84, and GM-Ab concentration and neutralizing ability increased further on day 182. In the context of long-term inhalation of GM-CSF, such as in the treatment of nontuberculous mycobacteria disease, the production of neutralizing antibodies may attenuate the effect of GM-CSF and pose a clinical challenge. In a previous report, GM-Ab was observed in 19 of 20 patients with metastatic colorectal carcinoma who had received subcutaneous administration of 250 μg of rhGM-CSF for 10 days every month for four months [45]. Further, the GM-Ab disappeared approximately 30 weeks after the last injection [45]. Taken the above into consideration, it is estimated that iBALT could be formed around day 28 and continue until the GM-Ab disappearance. If the efficacy of the drug is attenuated by the neutralizing antibodies, then discontinuation of treatment could be considered as an option. Alternatively, intermittent inhalation may serve as a strategy for avoiding the production of neutralizing antibodies.

The mechanism underpinning the extended retention of inhaled sargramostim in the lung and its transport to the BALT follicles remains unknown. Immunostaining using a sargramostim-specific monoclonal antibody showed that the presence of sargramostim in the follicles was not accompanied by its presence in either the epithelial lining fluid or the interstitium. Bronchoalveolar lavage (BAL) could potentially elucidate this process, although it was not performed in this nonclinical study to avoid any influence on the pathological tissue examination. A preliminary study, which was conducted separately, demonstrated that GM-CSF was easily detectable in BAL fluid one day after a single inhalation of *E. coli*-derived GM-CSF. Given that GM-CSF in the blood becomes undetectable within eight hours after a single inhalation [30], this may suggest that the kinetics of inhaled sargramostim in the lungs differ substantially from those in the blood and contribute to the accumulation of GM-CSF in the lungs following daily inhalation for seven days. Accordingly, the current regimen, which consists of 12 courses of seven-day inhalation followed by seven-day withdrawal, may need to be reconsidered. Even if inhaled GM-CSF accumulates in the lower respiratory tract, it may bind to the GM-CSF receptors of alveolar constituent cells and be internalized during the seven-day washout period. Further, GM-Ab emerging in the lower respiratory tract may bind to inhaled GM-CSF, and the resulting complex may bind to the Fc receptors of alveolar cells, including macrophages, and subsequently undergo cellular uptake to be metabolized.

This study serves as a reference for understanding the intrapulmonary dynamics of inhaled sargramostim and the behavior of sargramostim in the lower respiratory tract, particularly considering the formation of BALT and the role of lymphatic flow tissues in antibody production. Our findings suggest that inhaled sargramostim is retained in the lungs, is captured by the immune system, and contributes to the formation of antibodies.

Conclusions

Cynomolgus monkeys receiving 5–500 μg/kg/day of sargramostim via inhalation every other week for 26 weeks maintained good general condition. However, we observed a dose-dependent increase in the number and size of iBALT nodules in the peribronchiolar and alveolar regions. Since no iBALT proliferation was observed in the vehicle-treated monkeys, it appears to be sargramostim-specific. Because the sargramostim-binding cells were present in the iBALT but absent in the spleen and hilar lymph nodes, we propose that iBALT is the site of anti-sargramostim antibody production. Moreover, we observed a correlation between serum GM-Ab concentration and neutralizing ability with iBALT density in

the lungs, and between sargramostim accumulation in the germinal centers in iBALT nodules even one week after the cessation of inhalation. This suggests that antigen presentation might occur at the same site. The anti-sargramostim antibody that was produced suppressed the proliferation of alveolar macrophages in vitro when incubated in the presence of cynomolgus monkey GM-CSF. It also reduced peripheral blood leukocyte counts in vivo in the 100 and 500 μg/kg/day groups, suggesting its functional relevance in the body. We postulate that GM-Ab produced in hyperplastic iBALT may neutralize the effects of excessive sargramostim and contribute to the maintenance of homeostasis.

Abbreviations

aPAP	Autoimmune PAP
BALT	Bronchus-associated lymphoid tissue
ELISA	Enzyme-linked immunosorbent assay
GM-Ab	Anti-GM-CSF antibody
GM-CSF	Granulocyte-macrophage colony-stimulating factor
iBALT	Induced BALT
PAP	Pulmonary alveolar proteinosis
PBS	Phosphate-buffered saline
rhGM-CSF	Recombinant human GM-CSF

Supplementary Information

The online version contains supplementary material available at https://doi.org/10.1186/s12931-024-03003-w.

> Supplementary Material 1: Fig. 1. General condition of the 24 primates used in the study. The blue, green, brown, and red lines are the mean values for the 0, 5, 100, and 500 μg/kg/day sargramostim inhalation groups, respectively. The time courses of body weight (A, kg), heart. Rate (B, rate/min), and systolic blood pressure (C, mmHg) are graphically depicted. Fig. 2 . Gender differences in the number of iBALT depending on site or dose. Fig. 3 . Gender differences in the size of iBALT depending on site or dose. Table 1 . A generalized linear model with the number of iBALTs as the objective variable.

Author contributions

Ko. N., R.T., and Ka. N. designed the study. R.T., A.F., Ko. N., and Ka. N. managed the preclinical trial. N.K., R.O., S.Y., and T.T. analyzed the data. Ko. N., R.O., N.K., and R.T. wrote the manuscript with input from all the other authors.

Availability of data and materials

The data that support the findings of this study are not openly available due to reasons of sensitivity and are available from the corresponding author upon reasonable request. Data are located in controlled access data storage at Niigata University Medical and Dental Hospital.

Declarations

Ethics approval and consent to participate

All animal experiments were performed after approval by the Animal Experimental Ethics Board (approval no. 27-102-1) of Niigata University and the Institutional Animal Care and Use Committee (IACUC, approval no. 15091) of Ina Research (Nagano, Japan).

Consent for publication

Not Applicable.

Competing interests

The authors declare no competing interests.

Author details

[1]Health Administration Center, Tokyo Medical and Dental University, Tokyo, Japan. [2]Division of Molecular and Diagnostic Pathology, Histopathology Core Facility, Center for Research Promotion, Niigata University Graduate School of Medical and Dental Sciences, Niigata, Japan. [3]Division of Pioneering Advanced Therapeutics, Niigata University Medical and Dental Hospital, 1-754 Asahimachi-dori, Niigata 951-8520, Japan. [4]The Clinical and Translational Research Center, Niigata University Medical and Dental Hospital, Niigata, Japan. [5]Ina Research Inc, Nagano, Japan.

References

1. Walter MR, Cook WJ, Ealick SE, Nagabhushan TL, Trotta PP, Bugg CE. Three-dimensional structure of recombinant human granulocyte-macrophage colony-stimulating factor. J Mol Biol. 1992;224(4):1075–85. https://doi.org/10.1016/0022-2836(92)90470-5.
2. Campo I. The influence of genetics on therapeutic developments in pulmonary alveolar proteinosis. Curr Opin Pulm Med. 2019;25(3):294–9. https://doi.org/10.1097/MCP.0000000000000576.
3. Naito M. Macrophage differentiation and function in health and disease. Pathol Int. 2008;58(3):143–55. https://doi.org/10.1111/j.1440-1827.2007.02203.x.
4. Shima K, Arumugam P, Sallese A, Horio Y, Ma Y, Trapnell C, Wessendarp M, Chalk C, McCarthy C, Carey BC, Trapnell BC, Suzuki T. A murine model of hereditary pulmonary alveolar proteinosis caused by homozygous Csf2ra gene disruption. Am J Physiol Lung Cell Mol Physiol. 2022;322(3):L438–48. https://doi.org/10.1152/ajplung.00175.2021.
5. van de Laar L, Coffer PJ, Woltman AM. Regulation of dendritic cell development by GM-CSF: molecular control and implications for immune homeostasis and therapy. Blood. 2012;119(15):3383–93. https://doi.org/10.1182/blood-2011-11-370130.
6. Suzuki T, Trapnell BC. Pulmonary alveolar proteinosis syndrome. Clin Chest Med. 2016;37(3):431–40. https://doi.org/10.1016/j.ccm.2016.04.006.
7. Anderson PM, Markovic SN, Sloan JA, Clawson ML, Wylam M, Arndt CA, Smithson WA, Burch P, Gornet M, Rahman E. Aerosol granulocyte macrophage-colony stimulating factor: a low toxicity, lung-specific biological therapy in patients with lung metastases. Clin Cancer Res. 1999;5(9):2316–23.
8. Markovic SN, Suman VJ, Nevala WK, Geeraerts L, Creagan ET, Erickson LA, Rowland KM Jr, Morton RF, Horvath WL, Pittelkow MR. A dose-escalation study of aerosolized sargramostim in the treatment of metastatic melanoma: an NCCTG Study. Am J Clin Oncol. 2008;31(6):573–9. https://doi.org/10.1097/COC.0b013e318173a536.
9. Huffman JA, Hull WM, Dranoff G, Mulligan RC, Whitsett JA. Pulmonary epithelial cell expression of GM-CSF corrects the alveolar proteinosis in GM-CSF-deficient mice. J Clin Invest. 1996;97:649–55. https://doi.org/10.1172/JCI118461.
10. Reed JA, Ikegami M, Cianciolo ER, Lu W, Cho PS, Hull W, Jobe AH, Whitsett JA. Aerosolized GM-CSF ameliorates pulmonary alveolar proteinosis in GM-CSF-deficient mice. Am J Physiol. 1999;276:L556–63. https://doi.org/10.1152/ajplung.1999.276.4.L556.

11. Zsengellér ZK, Reed JA, Bachurski CJ, LeVine AM, Forry-Schaudies S, Hirsch R, Whitsett JA. Adenovirus-mediated granulocyte-macrophage colony-stimulating factor improves lung pathology of pulmonary alveolar proteinosis in granulocyte-macrophage colony-stimulating factor-deficient mice. Hum Gene Ther. 1998;9(14):2101–9. https://doi.org/10.1089/hum.1998.9.14-2101.

12. Tazawa R, Hamano E, Arai T, Ohta H, Ishimoto O, Uchida K, Watanabe M, Saito J, Takeshita M, Hirabayashi Y, Ishige I, Eishi Y, Hagiwara K, Ebina M, Inoue Y, Nakata K, Nukiwa T. Granulocyte-macrophage colony-stimulating factor and lung immunity in pulmonary alveolar proteinosis. Am J Respir Crit Care Med. 2005;171(10):1142–9. https://doi.org/10.1164/rccm.200406-716OC.

13. Wylam ME, Ten R, Prakash UB, Nadrous HF, Clawson ML, Anderson PM. Aerosol granulocyte-macrophage colony-stimulating factor for pulmonary alveolar proteinosis. Eur Respir J. 2006;27(3):585–93. https://doi.org/10.1183/09031936.06.00058305.

14. Tazawa R, Trapnell BC, Inoue Y, Arai T, Takada T, Nasuhara Y, Hizawa N, Kasahara Y, Tatsumi K, Hojo M, Ishii H, Yokoba M, Tanaka N, Yamaguchi E, Eda R, Tsuchihashi Y, Morimoto K, Akira M, Terada M, Otsuka J, Ebina M, Kaneko C, Nukiwa T, Krischer JP, Akazawa K, Nakata K. Inhaled granulocyte/macrophage-colony stimulating factor as therapy for pulmonary alveolar proteinosis. Am J Respir Crit Care Med. 2010;181(12):1345–54. https://doi.org/10.1164/rccm.200906-0978OC.

15. Tazawa R, Ueda T, Abe M, Tatsumi K, Eda R, Kondoh S, Morimoto K, Tanaka T, Yamaguchi E, Takahashi A, Oda M, Ishii H, Izumi S, Sugiyama H, Nakagawa A, Tomii K, Suzuki M, Konno S, Ohkouchi S, Tode N, Handa T, Hirai T, Inoue Y, Arai T, Asakawa K, Sakagami T, Hashimoto A, Tanaka T, Takada T, Mikami A, Kitamura N, Nakata K. Inhaled GM-CSF for pulmonary alveolar proteinosis. N Engl J Med. 2019;381(10):923–32. https://doi.org/10.1056/NEJMoa1816216.

16. Trapnell BC, Inoue Y, Bonella F, Morgan C, Jouneau S, Bendstrup E, Campo I, Papiris SA, Yamaguchi E, Cetinkaya E, Ilkovich MM, Kramer MR, Veltkamp M, Kreuter M, Baba T, Ganslandt C, Tarnow I, Waterer G, Jouhikainen T. IMPALA trial investigators. inhaled molgramostim therapy in autoimmune pulmonary alveolar proteinosis. N Engl J Med. 2020;383(17):1635–44. https://doi.org/10.1056/NEJMoa1913590.

17. Bosteels C, Van Damme KFA, De Leeuw E, Declercq J, Maes B, Bosteels V, Hoste L, Naesens L, Debeuf N, Deckers J, Cole B, Pardons M, Weiskopf D, Sette A, Weygaerde YV, Malfait T, Vandecasteele SJ, Demedts IK, Slabbynck H, Allard S, Depuydt P, Van Braeckel E, De Clercq J, Martens L, Dupont S, Seurinck R, Vandamme N, Haerynck F, Roychowdhury DF, Vandekerckhove L, Guilliams M, Tavernier SJ, Lambrecht BN. Loss of GM-CSF-dependent instruction of alveolar macrophages in COVID-19 provides a rationale for inhaled GM-CSF treatment. Cell Rep Med. 2022;15:100833. https://doi.org/10.1016/j.xcrm.2022.100833.

18. Paine R, Chasse R, Halstead ES, Nfonoyim J, Park DJ, Byun T, Patel B, Molina-Pallete G, Harris ES, Garner F, Simms L, Ahuja S, McManus JL, Roychowdhury DF. Inhaled sargramostim (recombinant human granulocyte-macrophage colony-stimulating factor) for COVID-19-associated acute hypoxemia: results of the phase 2, randomized, open-label trial (iLeukPulm). Mil Med. 2022;188(7–8):e2629-38. https://doi.org/10.1093/milmed/usac362.

19. Shimasaki S, Baba T, Ogura T, Akasaka K, Matsushima H, Izumi S, Takasaki J, Tsushima K, Kinouchi T, Kichikawa Y, Awashima M, Izumo T, Awano N, Nishimura N, Tazawa R, Mikami A, Kitamura N, Ishii H, Kurihara Y, Taniguchi M, Aikawa S, Okada M, Morita Y, Ishikawa Y, Ohinata A, Nakata K. Short-term inhalation of sargramostim with concomitant high-dose steroids does not hasten recovery in moderate COVID-19 pneumonia: a double-blind, randomised, placebo-controlled trial. Infect Dis (Lond). 2023;55(12):857–73. https://doi.org/10.1080/23744235.2023.2254380.

20. Thomson RM, Loebinger MR, Burke AJ, Morgan LC, Waterer GW, Ganslandt C. OPTIMA: an open-label, non-comparative pilot trial of inhaled molgramostim in pulmonary nontuberculous mycobacterial infection. Ann Am Thorac Soc. 2023. https://doi.org/10.1513/AnnalsATS.202306-532OC.

21. Pabst R, Gehrke I. Is the bronchus-associated lymphoid tissue (BALT) an integral structure of the lung in normal mammals, including humans? Am J Respir Cell Mol Biol. 1990;3(2):131–5. https://doi.org/10.1165/ajrcmb/3.2.131.

22. Hiller AS, Tschernig T, Kleemann WJ, Pabst R. Bronchus-associated lymphoid tissue (BALT) and larynx-associated lymphoid tissue (LALT) are found at different frequencies in children, adolescents and adults. Scand J Immunol. 1998;47(2):159–62. https://doi.org/10.1046/j.1365-3083.1998.00276.x.

23. Randall TD. Bronchus-associated lymphoid tissue (BALT) structure and function. Adv Immunol. 2010;107:187–241. https://doi.org/10.1016/B978-0-12-381300-8.00007-1.

24. Sato A, Chida K, Iwata M, Hayakawa H. Study of bronchus-associated lymphoid tissue in patients with diffuse panbronchiolitis. Am Rev Respir Dis. 1992;146(2):473–8. https://doi.org/10.1164/ajrccm/146.2.473.

25. Sato A, Hayakawa H, Uchiyama H, Chida K. Cellular distribution of bronchus-associated lymphoid tissue in rheumatoid arthritis. Am J Respir Crit Care Med. 1996;154(6 Pt 1):1903–7. https://doi.org/10.1164/ajrccm.154.6.8970384.

26. Suda T, Chida K, Hayakawa H, Imokawa S, Iwata M, Nakamura H, Sato A. Development of bronchus-associated lymphoid tissue in chronic hypersensitivity pneumonitis. Chest. 1999;115(2):357–63. https://doi.org/10.1378/chest.115.2.357.

27. Sato A. Basic and clinical aspects of bronchus-associated lymphoid tissue. Nihon Kokyuki Gakkai Zasshi. 2000;38(1):3–11.

28. Chvatchko Y, Kosco-Vilbois MH, Herren S, Lefort J, Bonnefoy JY. Germinal center formation and local immunoglobulin E (IgE) production in the lung after an airway antigenic challenge. J Exp Med. 1996;184(6):2353–60. https://doi.org/10.1084/jem.184.6.2353.

29. Uchida K, Nakata K, Trapnell BC, Terakawa T, Hamano E, Mikami A, Matsushita I, Seymour JF, Oh-Eda M, Ishige I, Eishi Y, Kitamura T, Yamada Y, Hanaoka K, Keicho N. High-affinity autoantibodies specifically eliminate granulocyte-macrophage colony-stimulating factor activity in the lungs of patients with idiopathic pulmonary alveolar proteinosis. Blood. 2004;103(3):1089–98. https://doi.org/10.1182/blood-2003-05-1565.

30. Nakano R, Nakagaki K, Itoh Y, Seino U, Ueda T, Tazawa R, Kitamura N, Tanaka T, Nakata K. Assay system development to measure the concentration of sargramostim with high specificity in patients with autoimmune pulmonary alveolar proteinosis after single-dose inhalation. J Immunol Methods. 2018;460:1–9. https://doi.org/10.1016/j.jim.2018.05.012.

31. Urano S, Kaneko C, Nei T, Motoi N, Tazawa R, Watanabe M, Tomita M, Adachi T, Kanazawa H, Nakata K. A cell-free assay to estimate the neutralizing capacity of granulocyte-macrophage colony-stimulating factor autoantibodies. J Immunol Methods. 2010;360(1–2):141–8. https://doi.org/10.1016/j.jim.2010.07.001.

32. Richmond I, Pritchard GE, Ashcroft T, Avery A, Corris PA, Walters EH. Bronchus associated lymphoid tissue (BALT) in human lung: its distribution in smokers and non-smokers. Thorax. 1993;48(11):1130–4. https://doi.org/10.1136/thx.48.11.1130.

33. Matsumoto R, Gray J, Rybkina K, Oppenheimer H, Levy L, Friedman LM, Khamaisi M, Meng W, Rosenfeld AM, Guyer RS, Bradley MC, Chen D, Atkinson MA, Brusko TM, Brusko M, Connors TJ, Luning Prak ET, Hershberg U, Sims PA, Hertz T, Farber DL. Induction of bronchus-associated lymphoid tissue is an early life adaptation for promoting human B cell immunity. Nat Immunol. 2023;24(8):1370–81. https://doi.org/10.1038/s41590-023-01557-3.

34. Dorman DC, Struve MF, Gross EA, Wong BA, Howroyd PC. Sub-chronic inhalation of high concentrations of manganese sulfate induces lower airway pathology in rhesus monkeys. Respir Res. 2005;6(1):121. https://doi.org/10.1186/1465-9921-6-121.

35. Ullenhag G, Bird C, Ragnhammar P, Frödin JE, Strigård K, Olsterborg A, Thorpe R, Mellstedt H, Wadhwa M. Incidence of GM-CSF antibodies in cancer patients receiving GM-CSF for Immunostimulation. Clin Immunol. 2001;99(1):65–74. https://doi.org/10.1006/clim.2000.4999.

36. Nei T, Urano S, Motoi N, Hashimoto A, Kitamura N, Tanaka T, Nakagaki K, Takizawa J, Kaneko C, Tazawa R, Nakata K. Memory B cell pool of autoimmune pulmonary alveolar proteinosis patients contains higher frequency of GM-CSF autoreactive B cells than healthy subjects. Immunol Lett. 2019;212:22–9. https://doi.org/10.1016/j.imlet.2019.05.013.

37. Uchida K, Nakata K, Suzuki T, Luisetti M, Watanabe M, Koch DE, Stevens CA, Beck DC, Denson LA, Carey BC, Keicho N, Krischer JP, Yamada Y, Trapnell BC. Granulocyte/macrophage-colony-stimulating factor autoantibodies and myeloid cell immune functions in healthy subjects. Blood. 2009;113(11):2547–56. https://doi.org/10.1182/blood-2009-05-155689.

38. Hayakawa H, Sato A, Imokawa S, Toyoshima M, Chida K, Iwata M. Bronchiolar disease in rheumatoid arthritis. Am J Respir Crit Care Med. 1996;154(5):1531–6. https://doi.org/10.1164/ajrccm.154.5.8912776.

Tazawa *et al. Respiratory Research*　　　(2024) 25:402

Page 16 of 16

39. Egashira R, Kondo T, Hirai T, Kamochi N, Yakushiji M, Yamasaki F, Irie H. CT findings of thoracic manifestations of primary Sjögren syndrome: radiologic-pathologic correlation. Radiographics. 2013;33(7):1933–49. https://doi.org/10.1148/rg.337125107.

40. Tanaka N, Newell JD, Brown KK, Cool CD, Lynch DA. Collagen vascular disease-related lung disease: high-resolution computed tomography findings based on the pathologic classification. J Comput Assist Tomogr. 2004;28(3):351–60. https://doi.org/10.1097/00004728-200405000-00009.

41. Raghu G, Remy-Jardin M, Ryerson CJ, Myers JL, Kreuter M, Vasakova M, Bargagli E, Chung JH, Collins BF, Bendstrup E, Chami HA, Chua AT, Corte TJ, Dalphin JC, Danoff SK, Diaz-Mendoza J, Duggal A, Egashira R, Ewing T, Gulati M, Inoue Y, Jenkins AR, Johannson KA, Johkoh T, Tamae-Kakazu M, Kitaichi M, Knight SL, Koschel D, Lederer DJ, Mageto Y, Maier LA, Matiz C, Morell F, Nicholson AG, Patolia S, Pereira CA, Renzoni EA, Salisbury ML, Selman M, Walsh SLF, Wuyts WA, Wilson KC. Diagnosis of hypersensitivity pneumonitis in adults. An official ATS/JRS/ALAT clinical practice guideline. Am J Respir Crit Care Med. 2020;202(3):e36-69. https://doi.org/10.1164/rccm.202005-2032ST.

42. Garg D, Mody M, Pal C, Patel P, Migliore C, Minerowicz C, Madan N. Follicular bronchiolitis: two cases with varying clinical and radiological presentation. Case Rep Pulmonol 2020 Jan. 2020;25:20204564587. https://doi.org/10.1155/2020/4564587.

43. Pipavath SJ, Lynch DA, Cool C, Brown KK, Newell JD. Radiologic and pathologic features of bronchiolitis. AJR Am J Roentgenol. 2005;185(2):354–63. https://doi.org/10.2214/ajr.185.2.01850354.

44. Weinman JP, Manning DA, Liptzin DR, Krausert AJ, Browne LP. HRCT findings of childhood follicular bronchiolitis. Pediatr Radiol. 2017;47(13):1759–65. https://doi.org/10.1007/s00247-017-3951-5.

45. Ragnhammar P, Friesen HJ, Frödin JE, Lefvert AK, Hassan M, Osterborg A, Mellstedt H. Induction of anti-recombinant human granulocyte-macrophage colony-stimulating factor (Escherichia coli-derived) antibodies and clinical effects in nonimmunocompromised patients. Blood. 1994;84(12):4078–87.

Publisher's note